Int. J. Dev. Biol. 70: 31-42 (2026)
https://doi.org/10.1387/ijdb.28997

THE INTERNATIONAL JOURNAL OF DEVELOPMENTAL BIOLOGY
www.intjdevbiol.com

Schlafen regulates gastrulation in *Xenopus laevis* early embryonic development and exhibits immune tissue-specific expression in adult frogs

GIANMATTEO VIT[1,2*], ALEXANDER HIRTH[3], BIANCA N. KRAFT[1], ANNA CAZZOLA[1], HARALD KLÜTER[2], CHRISTOF NIEHRS[4], ALWIN KRÄMER[1]

[1]*Clinical Cooperation Unit Molecular Hematology/Oncology, German Cancer Research Center (DKFZ) and Department of Internal Medicine V, University of Heidelberg, Heidelberg, Germany.*
[2]*Institute of Transfusion Medicine and Immunology, Medical Faculty Mannheim, Heidelberg University; German Red Cross Blood Service Baden-Württemberg | Hessen, Mannheim, Germany.*
[3]*Division of Molecular Embryology, DKFZ-ZMBH Alliance, Deutsches Krebsforschungszentrum (DKFZ), 69120 Heidelberg, Germany.*
[4]*Division of Molecular Embryology, DKFZ-ZMBH Alliance, Deutsches Krebsforschungszentrum (DKFZ), 69120 Heidelberg, Germany, and Institute of Molecular Biology (IMB), Mainz, Germany.*

ABSTRACT ***Schlafen*** **genes are conserved regulators of cell proliferation and play a pivotal role in immunity and host defence, yet their function during vertebrate development remains poorly understood. Here, we characterize the expression, phosphorylation dynamics, and function of the single** ***Schlafen*** **ortholog in** ***Xenopus laevis*** **(*slfn13*) during embryogenesis and in adult tissues. Slfn13 protein levels increase markedly around the mid-blastula transition/late blastula, with unphosphorylated Slfn13 predominating during gastrulation and neurulation, while phosphorylated Slfn13 (p-Slfn13) is more abundant during early cleavage stages. We found that Morpholino-mediated knockdown of Slfn13 in** ***Xenopus laevis*** **causes delayed blastopore lip formation, impaired blastopore closure, and severe gastrulation defects in a dose-dependent manner, indicating a non-redundant requirement for Slfn13 in early morphogenesis. We further analysed Slfn13 expression in adult** ***Xenopus laevis*****. Slfn13 is enriched in immune tissues and thymic tumour cell lines, with p-Slfn13 specifically detected in proliferative tumour-derived cells. Collectively, our findings reveal a previously unrecognized role for *slfn13* in gastrulation and support a conserved immune-associated expression pattern in adult frogs, expanding the functional landscape of Schlafen proteins across vertebrates.**

KEYWORDS: Schlafen, Xenopus, embryonic development, gastrulation, comparative immunology.

LABURPENA ***Schlafen*** **geneak zelulen proliferazioaren erregulatzaile kontserbatuak dira, eta funtsezko zeregina betetzen dute immunitatean eta ostalariaren defentsan; hala ere, oraindik ez dugu ondo ezagutzen zer funtzio betetzen duten ornodunen garapenean. Lan honetan,** ***Schlafen*****ek** ***Xenopus laevis*****en duen ortologo bakarraren (hots,** ***Slfn13*** **genearen) adierazpena, fosforilazio-dinamika eta funtzioa karakterizatu ditugu, bai enbriogenesian, bai ehun helduetan. Slfn13 proteina-kantitateak nabarmen egiten du gora tarteko blastulatik blastula berantiarrerako trantsizioan, gastrulazioan eta neurulazioan Slfn13-ren forma ez-fosforilatua nagusi izanik, eta forma fosforilatua (p-Slfn13), berriz, segmentazio-fase goiztiarretan. Konturatu ginen ezen, morfolino bidez** ***Xenopus laevis*****en** ***Slfn13*** **genea isilarazten bada, atzeratu egiten dela blastoporo-ezpainaren eraketa, blastoporoa ez dela behar bezala ixten, eta gastrulazioan dosiaren araberako akats larriak gertatzen direla; horrek guztiak agerian uzten du gene hori ezinbestekoa eta ez erredundantea dela morfogenesi goiztiarrerako.** ***Xenopus laevis*** **helduetan ere aztertu genuen** ***Slfn13*** **genearen adierazpena. Slfn13 kontzentrazioa handiagoa izaten da ehun immunitarioetan eta timoko tumoreetatik eratorritako lerro zelularretan, eta p-Slfn13 berariaz detektatzen da tumoreetatik eratorritako zelula proliferatiboetan. Oro har, gure aurkikuntzek erakusten dute** ***Slfn13*****-k orain arte ezezaguna zitzaigun funtzio bat betetzen duela gastrulazioan, eta igel helduetan immunitate-sistemari lotutako adierazpen-eredu kontserbatu bat duela. Aurkikuntza horiek zabaldu egiten dute ornodunetan Schlafen proteinek duten panorama funtzionala.**

HITZ-GAKOAK: Schlafen, Xenopus, enbrioi-garapena, gastrulazioa, immunologia konparatua.

***** ***Corresponding author:*** Gianmatteo Vit. gianmatteo.vit@medma.uni-heidelberg.de – https://orcid.org/0000-0002-3111-0769

Submitted: 26 February, 2026; Accepted: 19 June, 2026; Published online: 16 September, 2026.
ISSN 0214-6282 - eISSN 1696-3547 / © 2026 The authors

This is an open access article distributed under the terms and conditions of the *Creative Commons Attribution (CC BY-NC 4.0) license*

Introduction

Regulation of cell proliferation and differentiation during development is a fundamental requirement for morphogenesis and tissue homeostasis. These processes depend on tightly controlled regulatory networks that coordinate cell cycle progression with embryonic development. Disruption of such coordination can lead to developmental defects, pathological cell growth, and dysregulation of physiological processes.

Members of the *Schlafen* gene family have been implicated in several of these core biological processes. Originally identified in mice as regulators of thymocyte development, *Schlafen* genes are highly conserved and have been shown to be involved in the control of proliferation, hematopoietic differentiation, immune responses, and antiviral defence (de la Casa-Esperón, 2011; Fischietti *et al.,* 2022; Guillen Magaña *et al.,* 2025; Jo and Pommier, 2022; Li *et al.,* 2012; Schwarz *et al.,* 1998; Warsi *et al.,* 2022). Functional studies in murine models showed that ectopic expression or loss of individual Schlafen family members affects cell growth and T cell maturation, highlighting their involvement in cellular proliferation and differentiation (Geserick *et al.,* 2004; Schwarz *et al.,* 1998). In humans, Schlafen genes are differentially expressed across cell types and dynamically regulated by interferon signalling, suggesting a role in immune cell quiescence and activation (Condamine *et al.,* 2010; Puck *et al.,* 2015).

Evolutionarily, Schlafen genes form a clustered and conserved gene family that arose through multiple duplication events and subsequently diversified in a lineage-specific manner (de la Casa-Esperón, 2011; Jo and Pommier, 2022; Mordier *et al.,* 2025). This diversification has contributed to functional specialization, while concurrently challenging the assignment of discrete biological roles to individual paralogues due to sequence similarity and potential redundancy (de la Casa-Esperón, 2011; Mordier *et al.,* 2025). Several Schlafen proteins harbour helicase or RNase consensus motifs, supporting their role in nucleic acid metabolism or transcriptional processes, although the full spectrum of their molecular functions remains incompletely understood (Chen *et al.,* 2025; Podvalnaya *et al.,* 2023).

In our previous work, we addressed this complexity by focusing on SLFN5, a human Schlafen protein that is ubiquitously expressed in proliferating cells and its ortholog in *Xenopus laevis (X. laevis)*, Slfn13. Given that *Xenopus* harbours a single Schlafen gene, this organism provides a particularly powerful model to dissect the evolutionarily conserved mechanisms underlying Schlafen function. We demonstrated that SLFN5 protein levels oscillate during the cell cycle, peaking at G_2, and that SLFN5 is required for proper cell cycle progression and cellular viability. Mechanistically, SLFN5 interacts with the PP2A-B55α phosphatase complex in a phosphorylation-dependent manner, identifying SLFN5 as a CDK-regulated substrate whose phosphorylation and dephosphorylation are essential for normal proliferation (Vit *et al.,* 2022). We further extended these findings to *X. laevis*, showing that Slfn13, which shares high sequence homology with human SLFN5, is required for meiotic resumption of G_2-arrested oocytes and shows cyclic expression during the first cleavages, indicating an evolutionarily conserved role in cell cycle control (Figure 1) (Vit *et al.,* 2022).

Analysis of a published transcriptomic dataset (Peshkin *et al.,* 2015) indicates that *slfn13* transcript levels (transcript: XeXenL6RMv10021047m) are first detectable at the early gastrula stage (NF 10), reach a peak at late gastrula (NF 12), and subsequently decline gradually through later embryonic development towards tadpole stages (NF 33). While we previously established a conserved function for Schlafen proteins in regulating the G_2/M transition, it remains unclear whether Slfn13 also contributes to developmental processes beyond meiosis. Early vertebrate embryogenesis is characterized by rapid cleavage divisions and dramatic changes in cell cycle progression, such as the mid-blastula transition, during which zygotic transcription is activated and cell cycles lengthen (Newport and Kirschner, 1982; Hörmanseder *et al.,* 2013). Moreover, given the conserved immune functions of Schlafen proteins in vertebrates, we were interested in investigating whether Slfn13 contributes to immune regulation in the adult frog.

In the present study, we build on our previous findings to systematically investigate Slfn13 protein expression, phosphorylation dynamics and function throughout *Xenopus* embryogenesis and later developmental stages. By combining protein and RNA expression profiling in both embryonic and adult tissues with loss-of-function approaches, we uncovered a developmentally regulated role for Slfn13 that extends its conserved function in cell cycle control to embryonic morphogenesis and immune-associated processes in the adult animal.

Results

To extend our previous analysis of Slfn13 function and phosphorylation dynamics during oocyte maturation and early embryonic cell cycles (Vit *et al.,* 2022), we systematically examined Slfn13 protein expression from cleavage through neurula stages. This approach allowed us to map the temporal dynamics of phosphorylated (p-Slfn13) and unphosphorylated Slfn13 during early embryogenesis and to identify specific developmental stages where Slfn13 may play additional regulatory or developmental roles. To assess whether this developmental regulation is conserved in *Xenopus* species, we performed the same experiment using *Xenopus tropicalis* (*X. tropicalis*) embryos. Although a *slfn13* ortholog has not yet been annotated in *X. tropicalis*, Western blotting revealed a specific band consistent with Slfn13 (Figure 2A). CSF-arrested eggs (CSF, cytostatic factor, Cdk1-Cyclin B) were fertilized and embryos were collected at different developmental stages.

Whereas p-Slfn13 was the predominant protein variant following progesterone treatment during the first two cleavages in *X. laevis* (Vit *et al.,* 2022), unphosphorylated Slfn13 was the dominant form at later developmental stages until neurulation (Figure 2A). A marked increase in unphosphorylated Slfn13 signal was observed during blastula formation (NF 7), with a peak at the late blastula (NF 9) (Figure 2A-B). In contrast, p-Slfn13 showed a sharp peak at NF 6, and exhibited variable protein levels in later stages in both *X. laevis* and *X. tropicalis* (Figure 2A). Notably, the temporal protein level profile and phosphorylation-dependent mobility shift of Slfn13 in *X. laevis* closely mirrored those observed in *X. tropicalis* (Figure 2A-C). To assess



Fig. 1. Sequence alignment of *Xenopus laevis* Slfn13 and human SLFN5. Global pairwise sequence alignment of *X. laevis* Slfn13 (1-897 aa; UniProt-ID: Q6NTK7) and human SLFN5 (1-891 aa; UniProt-ID: Q08AF3) was generated using T-Coffee version 11.00. The alignment shows a T-Coffee consistency score of 940, indicating a highly reliable global alignment. Residue-specific consistency values reported at the top left of the figure (X.lae: 93; Human: 93; cons: 94) represent the average alignment consistency scores for each sequence and for the consensus line, respectively (Poirot *et al.,* 2003). In the consensus line, asterisks indicate identical residues, colons indicate strongly conserved substitutions, and periods indicate weakly conserved substitutions. Conserved residues are highlighted according to sequence conservation scores generated by T-Coffee/ESPript. A highly conserved region corresponding to the putative GTPase-like domain is highlighted by red bars. A conserved SWAVDV/L motif is indicated by cyan bars. The central helicase-associated region corresponding to the predicted DNA/RNA helicase domain is marked by purple bars, whereas the C-terminal UvrD-like helicase domain is highlighted by green bars.

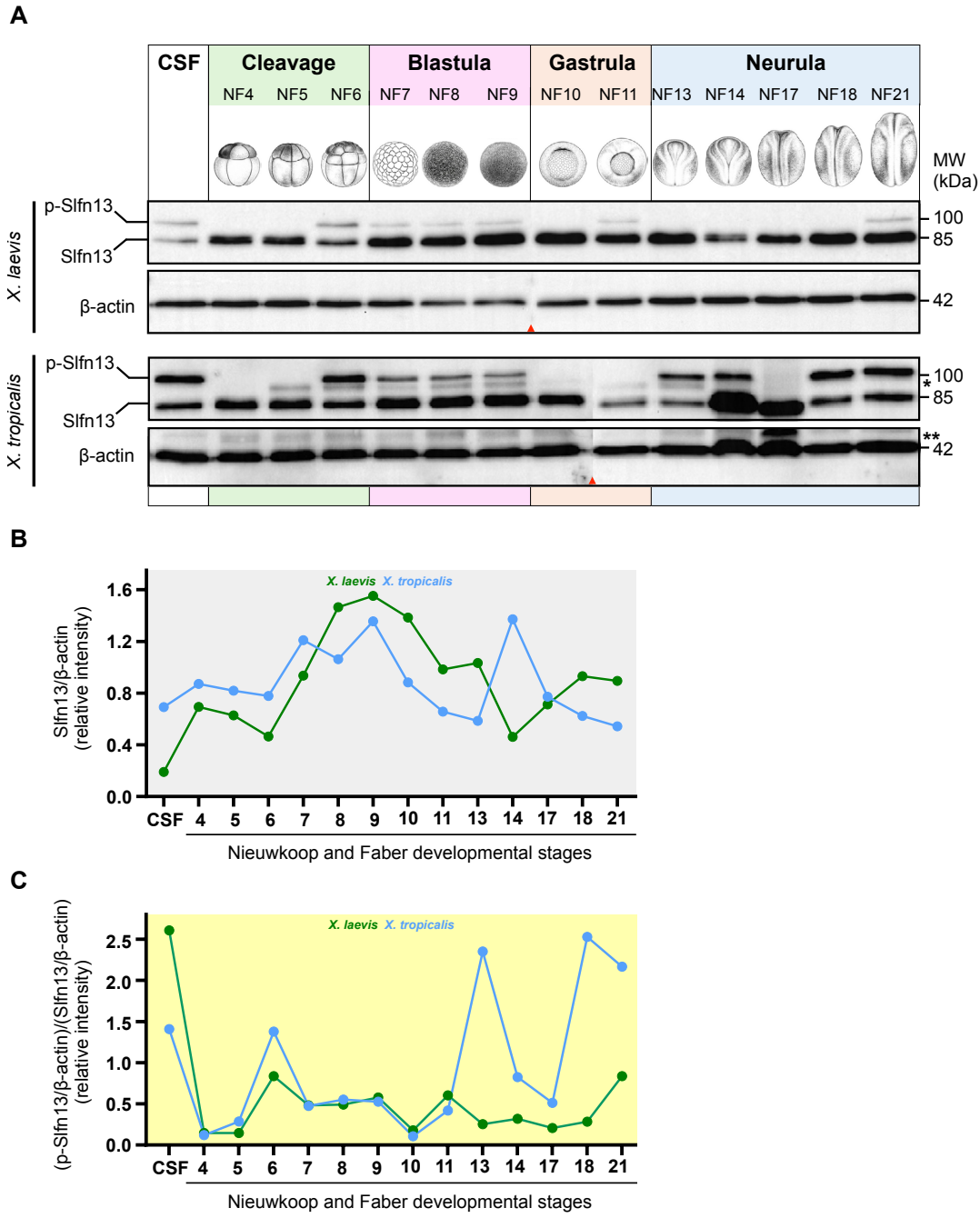


Fig. 2. Slfn13 and p-Slfn13 protein levels oscillate during *Xenopus* embryonic development from early cleavages until neurula formation. **(A)** Time course of Slfn13 and p-Slfn13 during *X. laevis* and *X. tropicalis* embryonic development. Slfn13 and p-Slfn13 protein level profile after fertilization shows an oscillating behaviour throughout embryonic development until the end of neurulation. A marked increase in protein amount is visible at the mid-blastula transition/late blastula (NF8-9). The Western blot shows a representative time course from three independent experiments using embryos obtained from independent fertilizations. For each developmental stage, five embryos were pooled for analysis as described in the figure. β-actin was used as loading control. p-Slfn13, phosphorylated x-Slfn13. NF, Nieuwkoop and Faber stages of *X. laevis* embryonic development (Nieuwkoop and Faber 1994). CSF, cytostatic factor. Drawings of *Xenopus* embryonic development are from Zahn *et al.*, 2022 (source: https://www.xenbase.org). Red arrowheads indicate the junctions between two juxtaposed Western blot membranes. *, uncharacterized Slfn13 band. **, non-specific signal. (**B**) Quantification of unphosphorylated Slfn13 protein levels normalized to β-actin (Slfn13/β-actin). Protein abundance is shown as relative intensity across developmental stages in *X. laevis* (green line) and *X. tropicalis* (blue line). Both species display a pronounced increase of Slfn13 at the mid-blastula transition/late blastula (NF8-9), followed by a gradual decline after neurulation. (**C**) Relative phosphorylation dynamics of Slfn13, expressed as the ratio between phosphorylated and unphosphorylated protein (p-Slfn13/β-actin)/(Slfn13/β-actin). In *X. tropicalis* (blue line), phosphorylation shows a prominent burst at NF6, comparable to *X. laevis*, and around NF13 and NF18. CSF, cytostatic factor. One representative time course was used for quantification (B-C).

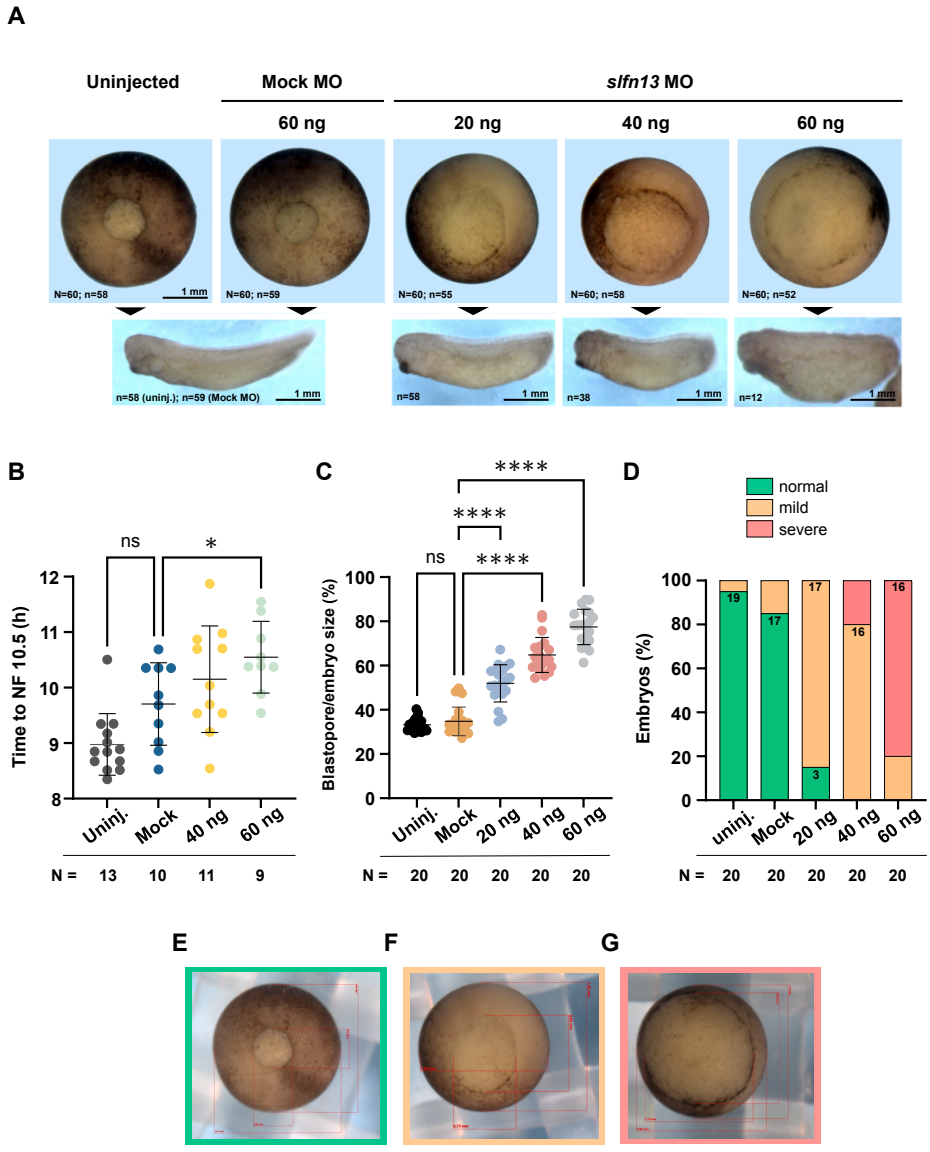


Fig. 3. Slfn13 depletion causes a dose-dependent delay and impairment of blastopore closure during embryonic development. **(A)** Injection of *X. laevis* embryos at the 4-cell stage (NF3) with increasing concentrations of antisense Morpholino (MO) impaired blastopore closure (upper panel) and embryonic development (lower panel). Standard control MOs were used for mock injections as controls. Embryos were collected at comparable developmental stages after injection, using uninjected controls as the reference (NF11.5-12 and late tailbud stages). The specificity of the antisense MOs oligomers was previously demonstrated by Western blotting (Vit *et al.,* 2022). MOs were injected into all four blastomeres at the 4-cell stage. The indicated amounts refer to the total quantity injected per embryo. Embryos show representative phenotypes for each experimental condition and are representative of three independent experiments. N, total number of embryos analysed; n, number of embryos showing the indicated phenotype. The number of embryos reaching the tailbud stage was 58/60 (uninjected), 59/60 (mock-injected), 58/60 (20 ng MO), 38/60 (40 ng MO), and 12/60 (60 ng MO), respectively. **(B)** Increasing concentrations of antisense MO caused a dose-dependent delay in blastopore lip formation. A significant delay (*, $p < 0.04$) was observed at 60 ng MO. The delay in blastopore lip formation was assessed by monitoring the time of appearance of the dorsal blastopore lip (NF10.5, onset of gastrulation) by time-lapse microscopy. ns, not statistically significant. Uninj., uninjected. The experiment was repeated independently three times. Data are presented as mean ± SD, with each dot representing one individual embryo. (**C–D**) Increasing concentrations of antisense MO induced dose-dependent defects in blastopore closure with a high degree of penetrance. A significant defect in blastopore closure (****, $p < 0.0001$) was observed in all experimental groups. The experiment was repeated independently three times. Numbers within the bars indicate the number of embryos displaying the corresponding phenotype for each experimental condition. Phenotypic analysis was performed at the time point when uninjected control embryos reached NF12. The blastopore-to-embryo size ratio was quantified using image analysis software by drawing measurement lines on microscopy images to determine both blastopore and embryo diameters. For each embryo, both the major and minor axes were measured for the blastopore and the embryo, and the final ratio was calculated based on the average values to account for biological asymmetry. Data are presented as mean ± SD, with each dot representing one individual embryo. (**E–G**) Representative examples of the phenotypic categories quantified in panel D. Blastopore closure defects were quantified by measuring the blastopore-to-embryo size ratio and classified as ≤0.4, 0.4–0.7, or ≥0.7, corresponding to normal blastopore closure (E), mild defects (F), or severe defects (G), respectively.

phosphorylation dynamics independently of total protein levels, we quantified the relative abundance of p-Slfn13 by normalizing it to unphosphorylated Slfn13. In *X. tropicalis*, the p-Slfn13/Slfn13 ratio shows two sharp peaks at NF 13 and NF 18, indicating transient phosphorylation events during early and late neurulation; in *X. laevis*, no comparable peaks were observed, and the p-Slfn13/Slfn13 ratio remained relatively low and stable throughout the same stages (Figure 2C). These results indicate that Slfn13 phosphorylation is dynamically regulated in a stage-specific and species-dependent manner during later embryogenesis.

To investigate whether and to what extent Slfn13 depletion affects embryonic development after fertilization, Morpholino (MO)-mediated Slfn13 depletion was performed in 4-cell stage embryos using an antisense MO whose efficacy and specificity were previously established (Vit *et al.,* 2022). Three experimental groups were injected with increasing concentrations of antisense MO, while injection of 60 ng standard control MO served as a control. MO-mediated Slfn13 depletion impaired blastopore closure and normal embryonic morphogenesis in a dose-dependent manner (Figure 3A and 4). At the highest MO concentration, severe blastopore closure defects frequently led to developmental arrest during gastrulation. To quantify the developmental delay, we measured by time-lapse microscopy the time required for the appearance of the dorsal blastopore lip, a key landmark of gastrulation onset (NF 10.5). At a dosage of 60 ng, *slfn13* MO-injected embryos exhibited a statistically significant delay of approximately 45 minutes in dorsal blastopore lip formation (Figure 3B and 4), consistent with the increased blastopore/embryo ratio observed at increasing MO concentrations (Figure 3C). More than 50% of embryos injected with 60 ng MO displayed severe blastopore closure defects and were unable to complete gastrulation (Figure 3D-G). Notably, very few embryos developed to the tailbud stage after injection with 60 ng MO while aberrant tailbud formation was observed in the remaining cases (Figure 3A). Embryos were scored based on developmental progression and gastrulation-associated phenotypes rather than survival time, as severely affected embryos frequently displayed heterogeneous developmental arrest and degeneration dynamics.

We next investigated *slfn13* expression in adult *X. laevis* organs and amphibian cell lines. Given the prominent role of *Schlafen* genes in mammalian and murine immune system development and function (Schwarz *et al.,* 1998; Geserick *et al.,* 2004; Berger *et al.,* 2010; Puck *et al.,* 2015; Vomhof-DeKrey *et al.,* 2019; Zhang *et al.,* 2024; Raglan and Kagan, 2024), we asked whether Slfn13 is associated with immune tissues in adult frogs. We performed whole-mount in situ hybridization (WISH) to explore the spatial distribution of *slfn13* transcripts at tailbud stage NF28. By WISH, *slfn13* exhibited prominent ventro-posterior expression, suggestive of ventral blood island pattern (Ciau-Uitz *et al.,* 2000) (Figure 5A). We therefore analysed mRNA and protein expression by real-time quantitative PCR (RT-qPCR) and Western blotting, respectively, in the ff-2, B3B7 and 15/0 *X. laevis* cell lines, previously characterized as thymic tumour cell lines (Robert *et al.,* 2003) and in primary tissues prepared from major immune and hematopoietic organs in *Xenopus* (thymus, spleen, kidney and liver), as well as non-immune organs (heart, lung and digestive tract). Consistent with our assumption, *slfn13* mRNA expression was detected at the highest level in all three T-cell lines, especially in B3B7 cells; among primary tissues, thymus, spleen, and kidney showed the highest mRNA levels, with expression in the thymus being highest among all cell lines and primary tissues tested. In contrast, *slfn13* expression in the liver (although variable), heart, and lung was detectable only at low levels, while expression in the digestive tract was barely measurable (Figure 5B-C). Consistent with mRNA results, Western blotting revealed strong Slfn13 protein expression in all cell lines, thymus and spleen. Notably, phosphorylated Slfn13 was specifically detected in tumour cell lines while unphosphorylated Slfn13 protein was expressed in thymus and spleen, suggesting a phosphorylation-dependent regulation of Slfn13 in different biological contexts (Figure 5D). Conversely, heart, lung and digestive tract extracts did not show detectable Slfn13 signals, suggesting higher Slfn13 levels in immune-related tissues (Figure 5E).

Discussion

In this study, we extended our previous characterization of Schlafen function beyond meiotic and mitotic cell cycle control and uncovered a role for *slfn13* during *Xenopus* embryogenesis as well as a preferential association with immune tissues in the adult frog. Our data demonstrate that Slfn13 protein expression is dynamically regulated during early development, peaks around the late blastula, and is required for proper gastrulation, identifying *Schlafen* as a direct or indirect regulator of early morphogenetic processes.

Expression of Slfn13 is developmentally regulated. The strong increase in protein amount around MBT/late blastula coincides with a fundamental developmental transition characterized by cell-cycle lengthening, activation of zygotic transcription, and the onset of large-scale cell movements. At these stages, unphosphorylated Slfn13 is the predominant form, whereas p-Slfn13, which we previously associated with meiotic resumption and cell cycle progression, shows an expression burst in the last cleavages (NF 6) in both *X. laevis* and *X. tropicalis*. This observation supports the idea that different phosphorylation states of Slfn13 may underlie distinct functional outputs, with p-Slfn13 potentially contributing to enhanced proliferative activity compared to the slowing of the cell cycle required for coordinated cell migration and tissue rearrangements during gastrulation (Brantley and Di Talia, 2021). Interestingly, we observed that in *X. tropicalis*, p-Slfn13 persists longer during embryonic development compared to *X. laevis* (NF 11-21), likely reflecting species-specific, spatially restricted regulatory events associated with neurulation, rather than global cell-cycle or growth-related phosphorylation. Another possible explanation for this difference may lie in the distinct genomic and developmental characteristics of the two species. *X. laevis* is an allotetraploid amphibian that originated through interspecific hybridization and retains extensive gene redundancy as a consequence of whole-genome duplication (Session *et al.,* 2016). In contrast, *X. tropicalis*, a diploid organism, exhibits faster embryonic cell cycles and a markedly shorter time to reach adulthood (Hirsch *et al.,* 2002). Polyploidy-associated gene dosage effects in *X. laevis* have been proposed to contribute to slower cell cycle progression and increased cell size, potentially through reduced dosage or loss of key cell cycle regulators, such

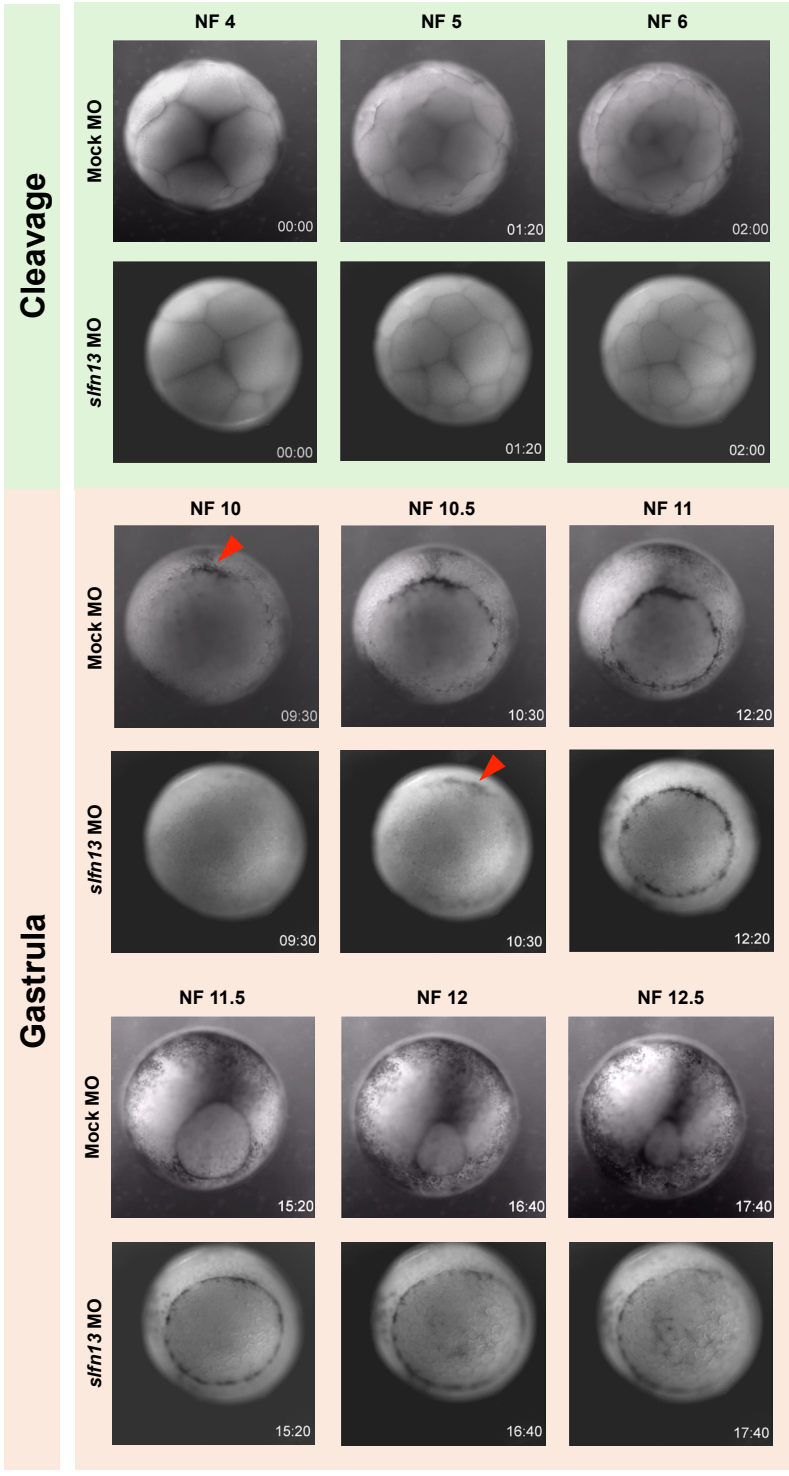


Fig. 4. Slfn13 depletion delays dorsal blastopore lip formation and impairs blastopore closure dynamics during gastrulation. Representative time-lapse analysis of *X. laevis* embryos injected at the 4-cell stage (NF 3) with either standard control Morpholino (Mock MO) or 40 ng antisense *slfn13* Morpholino (*slfn13* MO). Embryonic development was continuously monitored by time-lapse imaging from early cleavage stages through gastrulation to assess blastopore closure dynamics over time. Upper panels show cleavage stages (NF 4-6), where no gross morphological differences were observed between mock and *slfn13* MO-injected embryos. Lower panels illustrate gastrulation stages (NF 10-12.5), highlighting a delayed onset of the dorsal blastopore lip formation and impaired progression of blastopore closure in *slfn13* MO-injected embryos compared to controls. Red arrowheads indicate the site of the dorsal blastopore lip formation. The following numbers of embryos were analysed: uninjected control (n = 13), Mock MO (n = 10), 40 ng *slfn13* MO (n = 11), and 60 ng *slfn13* MO (n = 9). Developmental stages are indicated according to Nieuwkoop and Faber (NF), and time stamps (h:min) denote time after the start of imaging following injection.

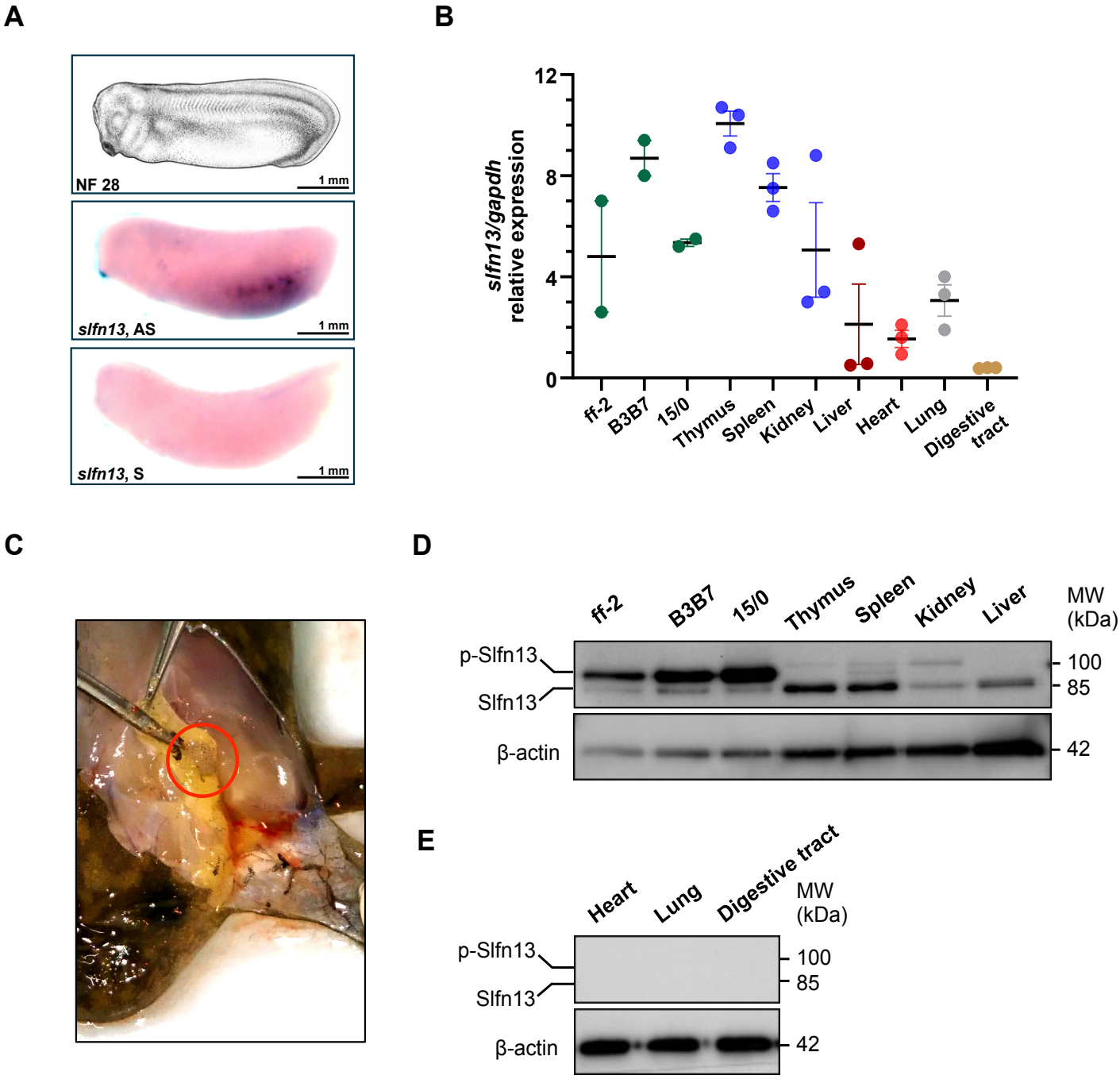


Fig. 5. *slfn13* gene expression and protein levels are enriched in lymphoid cells and organs in adult frogs. **(A)** Whole-mount in situ hybridization for *slfn13* mRNA revealed ventral localization of the digoxigenin-labelled antisense (AS) probe in NF 28 tailbud embryos, with signal accumulation in a pattern resembling the ventral blood island. A complementary sense (S) probe was used as a negative control. The embryo shown is representative of three independent experiments (n = 10 embryos per experiment). **(B)** *Xenopus* thymic tumor cell lines (ff-2, B3B7, and 15/0) and organs dissected from adult frogs were processed to obtain single-cell extracts. Quantitative real-time PCR was performed to assess *slfn13* mRNA expression. Data are presented as mean ± SD. *gapdh* was used as a housekeeping gene. Organs from three frogs were pooled for each experiment. Organs were isolated according to Jonas-Closs and Peshkin (Jonas-Closs and Peshkin, 2024). **(C)** Representative image of the thymus dissected from an adult *Xenopus laevis*. The thymus is a paired, small, pale, and semi-translucent organ located in the anterior cervical region, lateral to the pharynx and anterior to the heart. It lies superficially beneath the skin, adjacent to connective tissue and blood vessels. Fine forceps indicate the position of the thymic lobes following removal of the overlying tissue. **(D)** Western blotting of Slfn13 in thymic tumour cell lines (ff-2, B3B7, and 15/0) and adult *Xenopus* organs. β-actin was used as a loading control. p-Slfn13, phosphorylated Slfn13. **(E)** Slfn13 detection across additional adult tissues highlights the absence of detectable Slfn13 signal in heart, lung, and digestive tract extracts, in contrast to immune-related tissues and cell lines. Organs from at least 10 frogs were pooled and homogenized for Western blot analysis (D-E).

as components of the Cdk-activating kinase complex (Session *et al.,* 2016). In this context, the more pronounced and prolonged presence of p-Slfn13 at later stages in *X. tropicalis* may reflect a higher demand for cell cycle-promoting activity in a developmental program characterized by rapid proliferation and shorter interphases. Conversely, the predominance of unphosphorylated Slfn13 in *X. laevis* may be consistent with a developmental strategy that favours prolonged cell cycle slowing to accommodate extensive morphogenetic movements in a larger, polyploid embryo. Although speculative, this interpretation raises the possibility that Schlafen phosphorylation dynamics are tuned to species-specific cell cycle kinetics and growth peculiarities.

Morpholino-mediated depletion of Slfn13 resulted in delayed blastopore lip formation and closure, and severe gastrulation defects in a dose-dependent manner. These phenotypes highlight a non-redundant requirement for Slfn13 during early embryonic development and suggest that Schlafen function is not limited to cell cycle regulation, but is also essential for morphogenetic movements. Whether these defects arise from altered cell cycle dynamics, impaired cell migration, or a combination of both remains to be determined.

In adult *Xenopus*, we observed an enrichment of Slfn13 expression in immune-related tissues and thymic tumour cell lines, mirroring the immune-associated expression patterns described for Schlafen genes in mammals. The detection of p-Slfn13 specifically in tumour cell lines, but not in primary immune organs, further suggests a context-dependent regulation of Schlafen activity, potentially linked to sustained proliferation or transformation status.

Although we advanced our understanding of Slfn13, notable limitations of the present study need to be acknowledged. First, the observed protein expression in *X. tropicalis* is not supported by the presence of a previously annotated *slfn13* gene in this species. To further address the possibility of additional *Slfn* family members or an unannotated *Slfn13* ortholog in *X. tropicalis*, we performed *in silico* analyses using current genome assemblies available in Ensembl and NCBI. BLAST searches using both nucleotide and amino acid sequences of *X. laevis Slfn13* identified only very short regions of partial similarity in the *X. tropicalis* genome, without evidence of a full-length coding sequence or a closely related protein ortholog. While *Slfn13* is not annotated in current databases for *X. tropicalis*, these findings suggest that a highly diverged ortholog may exist. Nevertheless, the specific band detected by Western blotting closely matches the signals observed in *X. laevis* for both Slfn13 and p-Slfn13, supporting the robustness of our conclusions. Second, our loss-of-function analysis relies on MO-mediated knockdown in *X. laevis*, which leaves maternal protein unaffected, preventing us from investigating the full role that the protein may play in early development. Finally, we acknowledge that rescue experiments using MO-insensitive mRNA were not included in this study, which would have provided an additional level of validation of phenotypic specificity; nevertheless, together with the previously established specificity of Slfn13 knockdown (Vit *et al.,* 2022) and the reproducibility of the observed dose-dependent phenotypes, our findings remain robust.

In conclusion, our study reveals a previously unrecognized role for *slfn13* in coordinating early embryonic development and provides the evidence for immune-associated expression of Schlafen in adult frogs. Together, these findings expand the functional landscape of Schlafen proteins and open new avenues for understanding how phosphorylation-dependent regulation of Schlafen contributes to developmental timing and morphogenesis in vertebrates.

Materials and methods

Amphibian cell culture

Amphibian cell lines (ff-2, B3B7 and 15/0) were purchased from Jacques Robert, Xenopus laevis Research Resource for Immunobiology, University of Rochester, Rochester, USA. Cells were maintained at 26 °C in a humidified 6% CO_2 incubator. Cells were cultured in Amphibian Serum-Free (ASF) medium prepared from Mammalian Serum-Free basic medium (MSF) and supplemented with 10% fetal bovine serum (FBS) as follows: 200 mL MSF (IMDM powder 1 package, 10 mL Penicillin–Streptomycin, 10 mL non-essential amino acids, 10 mL insulin, 1 mL 2-mercaptoethanol, 3 mL Primatone, 3.02 g $NaHCO_3$ per liter) was combined with 60 mL distilled water, 25 mL FBS, 5 mL Penicillin–Streptomycin, and 500 µL kanamycin. The pH of the final medium was adjusted to 7.0 with 10 N NaOH, and the medium was sterile-filtered through a 0.2 µm filter and stored at 4 °C until use. For washing steps, Amphibian Serum-Free medium without additives was prepared using 200 mL MSF + 60 mL distilled water and filtered through a 0.2 µm filter. Amphibian phosphate-buffered saline (APBS) was adjusted to a pH of 7.7 with 10 N NaOH. APBS was sterile-filtered through a 0.2 µm filter as needed. All media and APBS (2.7 mM KCl, 0.15 mM KH_2PO_4, 103 mM NaCl, 0.7 mM $Na_2PO_4 \cdot 2H_2O$, pH 7.5) were adapted to the amphibian osmolarity of ~190 mOsm/kg. Cell contamination tests were performed by Multiplexion GmbH (Friedrichshafen, Germany).

X. laevis and *X. tropicalis* maintenance and husbandry

Xenopus experiments were approved by the state review board of Baden-Württemberg (Germany) and performed according to federal and institutional guidelines. Animals were obtained from EXRC (Portsmouth, UK) and Nasco (Fort Atkinson, USA) and kept in a *Xenopus* facility designed by Tecniplast at 18 °C with a light/dark cycle of 12/12 h. *Xenopus* males were killed in a bath of MS-222 (Sigma-Aldrich).

Immunoblotting

For Western blotting, five embryos were pooled per sample, flash frozen in liquid nitrogen and stored at −80 °C until use. *Xenopus* cells, embryos and adult tissues were lysed in lysis buffer (50 mM Tris/HCl, pH 7.4, 1 mM NaCl, 1 mM EDTA, 0.25% sodium deoxycholate, 1% NP-40) supplemented with protease and phosphatase inhibitor cocktail (Roche). If required, benzonase nuclease (Millipore Merk) was added at a concentration of 50 U/ml in order to dissolve DNA residues. Lysates were resolved on 10% acrylamide gels as desribed by Thomas and Kornberg (Thomas and Kornberg, 1975) and proteins were blotted on PVDF membrane. Following antibodies were used: 1. Anti-Slfn13 monoclonal antibody was raised in mouse as previously described (Vit *et al.,* 2022). 2. Anti-β-actin-HRP mouse

monoclonal antibody was purchased from Santa Cruz Biotechnology, Inc. (Cat. sc-47778). 3. Mouse TrueBlot™ HRP-conjugated secondary antibody was purchased from Rockland, Inc. (Cat. 18-8817-33).

Fertilization and collection of *X. laevis* embryos

Females of *X. laevis* were primed with 600 U of human chorionic gonadotropin (hCG, Genaxxon) into the dorsal lymph sac. After 24 h, eggs were gently harvested from the frogs by manual squeezing and subsequently prepared for fertilization. A testis from an adult *Xenopus* male was finely macerated with scissors and forceps to obtain sperms which were then pipetted on eggs, incubated for 3 min, flooded with 0.1× Barth (8.8 mM NaCl, 0.1 mM KCl, 0.24 mM $NaHCO_3$, 0.082 mM MgSO4 · $7H_2O$, 0.033 mM $Ca(NO_3)2 \cdot 4H_2O$, 0.041 mM $CaCl_2 \cdot 2H_2O$, 1 mM HEPES (pH7.6)) and incubated for 15 min after which successful fertilization was assessed by the characteristic post-fertilization reorientation of the embryo. Embryos were subsequently dejellied using 2% cysteine (Sigma-Aldrich) dissolved in water and the pH adjusted with NaOH to 7.8-8.0. After dejellying, embryos were washed three times in 0.1× Barth, three times in 0.3× Barth, transferred to a Petri dish and cultured to the corresponding stage at 20-22 °C in 0.1× Barth solution. Solution was changed four times a day to allow a normal development of the embryos. From stage NF 40 tadpoles were fed with TetraMin Baby dust feed for fishes. Embryos were staged according to Nieuwkoop and Faber Normal Table of Xenopus laevis (Daudin) (Nieuwkoop and Faber, 1994) under a microscope with epi-illumination.

Injection of *X. laevis* embryos

Embryos were injected at NF 3 with 20, 40 or 60 ng of antisense Morpholino (purchased from Gene Tools, LLC, Philomath, Oregon, USA) targeting the 5' UTR of *slfn13* (5'-ATGAAAACTATTCCTGTCTGTCCAG-3'). The control group was injected with 60 ng of standard control Morpholino (5'-CCTCTTACCTCAGTTACAATTTATA-3'). Morpholinos were injected into all four blastomeres at the 4-cell stage. The indicated Morpholino amounts represent the total quantity injected per embryo, equally distributed among the four blastomeres. Morpholino designs were BLASTed to check for possible cross-identification of other gene sequences. Microinjection was performed using a Pico-Injector PLI-100, Harvard Instruments.

Whole-mount *in situ* hybridization (WISH)

Slfn13 (Slfn13.L) ORF was purchased from GE Healthcare Xenopus Genome Collection (XGT) (Clone ID: 6635594) and cloned into pCS2+ expression vector. From the full-length *X. laevis* ORF, a 700-bp DNA fragment was amplified by PCR for RNA probe synthesis. RNA probe synthesis and digoxigenin-UTP (DIG) labelling were performed by *in vitro* transcription using SP6 and T7 RNA polymerases with the DIG RNA Labelling Kit (SP6/T7) (Roche Applied Science; Cat. 11175025910), according to the manufacturer's instructions. RNA gel electrophoresis of DIG-labelled probes was performed to assess purity of the probe and DIG-RNA labelling efficiency was determined by Dot blot on a nylon membrane by nucleic acid cross-linking with UV-light and subsequent incubation with anti-DIG antibody (1:1000) for 30 minutes and detected by BM purple on membrane. Labelled probes were aliquoted at −25 °C until use. WISH was performed as follows: embryos were fixed in MEMFA (1×MEM buffer containing 0.21 M MOPS pH 7.4, 4 mM EGTA, and 2 mM $MgSO_4$, supplemented with 3.7% formaldehyde) for 1 h at room temperature or overnight at 4 °C, bleached by illumination for 60 min in bleaching solution (80% methanol (MeOH), 10% formamide, and 10% hydrogen peroxide (H_2O_2, 30%)), and again fixed in MEMFA for 30 min at room temperature. Embryos were rehydrated through a graded ethanol series (100%, 75%, 50%, 25%) and washed in PTW (1×PBS containing 0.1% Tween-20 in DEPC-treated water). Proteinase K treatment (10 µg/mL) was performed for 30 min, followed by two washes in 0.1 M triethanolamine (TEA) and acetylation with acetic anhydride (5 µL per 2 mL TEA, twice). Embryos were washed in TBST (1×TBS supplemented with 0.1% Tween-20 in DEPC-treated water) and refixed in freshly prepared MEMFA for 60 min, followed by extensive TBST washes. For hybridization, embryos were equilibrated twice in hybridization buffer (HB, 50% formamide, 5×SSC (composition below), 1 mg/mL torula RNA, 50 µg/mL heparin, 1×Denhardt's solution, 0.05% Tween-20, 0.05% CHAPS, and 5 mM EDTA) and preincubated at 60 °C for 6-7 h. DIG-labelled antisense or sense RNA probes (1 µg/mL) were denatured at 85 °C for 5 min, added to the embryos, and hybridized overnight at 60 °C. After hybridization, embryos were washed in HB, followed by two washes in 2×SSC (1×SSC consisting of 150 mM NaCl and 15 mM sodium citrate (pH 7.0) in DEPC-treated water) with 0.05% Tween-20 at 60 °C. RNA digestion was performed to reduce background by incubating embryos twice for 30 min in 2×SSC containing RNase A (2 µg/mL) and RNase T1 (0.1 µg/mL) at 37 °C, followed by washes in 2×SSC and high-stringency washes in 0.2×SSC with 0.05% Tween-20 at 60 °C. Embryos were then washed in TBST at room temperature. For detection, embryos were blocked in blocking buffer, consisting of 1× blocking reagent (BMB, Roche), 10% goat serum, and 0.5% Tween-20 in DEPC-treated water, for 1 h at room temperature and incubated with anti-DIG alkaline phosphatase–conjugated antibody (Cat. 11093274910, Roche) for 4 h at room temperature or overnight at 4 °C. After extensive washing in TBST, colorimetric detection was performed using NBT/BCIP in AP buffer (100 mM Tris-HCl (pH 9.5), 50 mM $MgCl_2$, 100 mM NaCl, and 0.1% Tween-20 in DEPC-treated water) at 4 °C in the dark until the desired signal intensity was reached. The reaction was stopped by washing in TBST, and embryos were refixed in MEMFA containing 0.1% Tween-20 for 1-2 h at room temperature or overnight at 4 °C. Embryos were stored in 20% ethanol at −20 °C. All solutions were prepared using DEPC-treated water unless otherwise indicated.

Real-time quantitative PCR (qPCR)

Total RNA was extracted using TRIzol Reagent (Ambion, Cat. 15596-018) following the manufacturer's instructions. Samples were homogenized in TRIzol, phase-separated with 100% chloroform, and RNA was precipitated with isopropanol. The RNA pellet was washed with 80% ethanol, air-dried, and resuspended in RNase-free water. RNA concentration and purity were determined using a NanoDrop spectrophotometer. cDNA was synthesized using random primers with the Roche cDNA synthesis kit (Cat. 5081955001) according to the man-

ufacturer's protocol. qPCR was performed on a Roche Light-Cycler 480 using the LightCycler® 480 SYBR Green I Master, Roche (Cat. 04707516001). Reactions were run in technical triplicates together with no-template controls. Thermal cycling conditions were: pre-incubation at 95 °C for 5 min, followed by 45 cycles of 95 °C for 10 s, 60 °C for 10 s, 72 °C for 15 s. A melting curve was performed at the end of the run (95 °C for 5 s, 60 °C for 1 min, cooling). Following primer sequences were used for *slfn13*: FWD: 5´-TCCATCCAGTACCTGCCTAAGCTG-3´; REV: 5´-CGCACAAAGTGACTTTTTTCATAAAGGAC-3´. Gene ID: 6252126 (XORFeome v1.0). Relative expression was calculated using the ΔΔCt method and normalized to *gapdh*. Following primer sequences were used for *gapdh*: FWD: 5´-CACAAGAC-CAGGTTGTCTCCACT-3´; REV: 5´-GGCTGTAGCCGCATTCAT-TATCA-3´.

Time-lapse microscopy

MO injected embryos were monitored during gastrulation with images taken every two minutes using the AxioCam MRc 5 microscope (Zeiss).

Quantification and statistical analysis

Statistical analyses were performed using GraphPad Prism 10 (San Diego, CA). Data are presented as mean ± SD. Statistical significance was determined using one-way ANOVA. p-values are reported in the figure legends. Protein bands were quantified using Fiji/ImageJ. Band intensity was measured as integrated density after subtracting local background. Values were normalized to the corresponding loading control (β-actin). Relative protein levels were calculated by setting the control sample to 1.

Conflict of interest

The authors have nothing to disclose.

References

BRANTLEY, S. E., & DI TALIA, S. (2021). Cell cycle control during early embryogenesis. *Development (Cambridge, England)*, *148*(13), dev193128. https://doi.org/10.1242/dev.193128

CHEN, S. M., MA, L., WANG, Z., LI, Q. J., ZHOU, R., WANG, J., DING, J. W., ZHAO, J. Y., YI, D. R., ZHANG, Y. X., GUO, S. S., WANG, X. L., LI, X. Y., LIU, Z. L., & CEN, S. (2025). SLFN14 functions as a P-TEFb inhibitor to modulate the transcription of HIV-1 and cellular genes. *Science advances*, *11*(51), eadt7982. https://doi.org/10.1126/sciadv.adt7982

CIAU-UITZ, A., WALMSLEY, M., & PATIENT, R. (2000). Distinct origins of adult and embryonic blood in *Xenopus*. *Cell*, *102*(6), 787-796. https://doi.org/10.1016/s0092-8674(00)00067-2

CONDAMINE, T., LE LUDUEC, J. B., CHIFFOLEAU, E., BÉRIOU, G., LOUVET, C., HESLAN, M., TILLY, G., & CUTURI, M. C. (2010). Characterization of Schlafen-3 expression in effector and regulatory T cells. *Journal of leukocyte biology*, *87*(3), 451-456. https://doi.org/10.1189/jlb.0609410

DE LA CASA-ESPERÓN, E. (2011). From mammals to viruses: the Schlafen genes in developmental, proliferative and immune processes. *Biomolecular concepts*, *2*(3), 159-169. https://doi.org/10.1515/bmc.2011.018

FISCHIETTI, M., ECKERDT, F., PEREZ, R. E., GUILLEN MAGAÑA, J. N., MAZEWSKI, C., HO, S., GONZALEZ, C., STREICH, L. D., BEAUCHAMP, E. M., HEIMBERGER, A. B., BARAN, A. H., YUE, F., JAMES, C. D., & PLATANIAS, L. C. (2022). SLFN11 negatively regulates non-canonical NFkB signaling to promote glioblastoma progression. *Cancer research communications*, *2*(9), 966-978. https://doi.org/10.1158/2767-9764.crc-22-0192

GESERICK, P., KAISER, F., KLEMM, U., KAUFMANN, S. H., & ZERRAHN, J. (2004). Modulation of T cell development and activation by novel members of the Schlafen (slfn) gene family harbouring an RNA helicase-like motif. *International immunology*, *16*(10), 1535-1548. https://doi.org/10.1093/intimm/dxh155

GUILLEN MAGAÑA, J. N., ZANNIKOU, M., BARAN, A., SMALL, S., SCHIEBER, M., SCHIPMA, M. J., BARTOM, E. T., KOCHERGINSKY, M., SALEIRO, D., BEAUCHAMP, E. M., ECKERDT, F., & PLATANIAS, L. C. (2025). *Schlafen* 12 Modulation and Targeting in Acute Myeloid Leukemia. *Cancer research communications*, *5*(11), 2012-2024. https://doi.org/10.1158/2767-9764.CRC-25-0283

HIRSCH, N., ZIMMERMAN, L. B., & GRAINGER, R. M. (2002). *Xenopus,* the next generation: *X. tropicalis* genetics and genomics. *Developmental dynamics: an official publication of the American Association of Anatomists*, *225*(4), 422-433. https://doi.org/10.1002/dvdy.10178

HÖRMANSEDER, E., TISCHER, T., & MAYER, T. U. (2013). Modulation of cell cycle control during oocyte-to-embryo transitions. *The EMBO journal*, *32*(16), 2191-2203. https://doi.org/10.1038/emboj.2013.164

JONAS-CLOSS, R. A., & PESHKIN, L. (2024). Techniques for Rapidly Sampling Six Crucial Organs in Adult *Xenopus*. *Journal of visualized experiments: JoVE*, (204), 10.3791/66489. https://doi.org/10.3791/66489

LI, M., KAO, E., GAO, X., SANDIG, H., LIMMER, K., PAVON-ETERNOD, M., JONES, T. E., LANDRY, S., PAN, T., WEITZMAN, M. D., & DAVID, M. (2012). Codon-usage-based inhibition of HIV protein synthesis by human *schlafen* 11. *Nature*, *491*(7422), 125-128. https://doi.org/10.1038/nature11433

MORDIER, J., FRAISSE, M., COHEN-TANNOUDJI, M., & MOLARO, A. (2025). Recurrent Evolutionary Innovations in Rodent and Primate *Schlafen* Genes. *Genome biology and evolution*, *17*(10), evaf172. https://doi.org/10.1093/gbe/evaf172

NEWPORT, J., & KIRSCHNER, M. (1982). A major developmental transition in early *Xenopus* embryos: II. Control of the onset of transcription. *Cell*, *30*(3), 687-696. https://doi.org/10.1016/0092-8674(82)90273-2

NIEUWKOOP, P. D., & FABER, J. (1994). Normal table of *Xenopus laevis* (Daudin): A systematical and chronological survey of the development from the fertilized egg till the end of metamorphosis. New York: Garland Publishing.

PESHKIN, L., WÜHR, M., PEARL, E., HAAS, W., FREEMAN, R. M., JR, GERHART, J. C., KLEIN, A. M., HORB, M., GYGI, S. P., & KIRSCHNER, M. W. (2015). On the Relationship of Protein and mRNA Dynamics in Vertebrate Embryonic Development. *Developmental cell*, *35*(3), 383-394. https://doi.org/10.1016/j.devcel.2015.10.010

PODVALNAYA, N., BRONKHORST, A. W., LICHTENBERGER, R., HELLMANN, S., NISCHWITZ, E., FALK, T., KARAULANOV, E., BUTTER, F., FALK, S., & KETTING, R. F. (2023). piRNA processing by a trimeric *Schlafen*-domain nuclease. *Nature*, *622*(7982), 402-409. https://doi.org/10.1038/s41586-023-06588-2

POIROT, O., O'TOOLE, E., NOTREDAME, C. TCOFFEE@IGS: A WEB SERVER FOR COMPUTING, EVALUATING AND COMBINING MULTIPLE SEQUENCE ALIGNMENTS. *NUCLEIC ACIDS RES*. 2003 JUL 1;31(13):3503-6. https://doi: 10.1093/nar/gkg522.

PUCK, A., AIGNER, R., MODAK, M., CEJKA, P., BLAAS, D., & STÖCKL, J. (2015). Expression and regulation of *Schlafen* (SLFN) family members in primary human monocytes, monocyte-derived dendritic cells and T cells. *Results in immunology*, *5*, 23-32. https://doi.org/10.1016/j.rinim.2015.10.001

ROBERT, J., GANTRESS, J., COHEN, N., & MANIERO, G. D. (2004). *Xenopus* as an experimental model for studying evolution of hsp--immune system interactions. *Methods (San Diego, Calif.)*, *32*(1), 42-53. https://doi.org/10.1016/s1046-2023(03)00186-5

SESSION, A. M., UNO, Y., KWON, T., CHAPMAN, J. A., TOYODA, A., TAKAHASHI, S., FUKUI, A., HIKOSAKA, A., SUZUKI, A., KONDO, M., VAN HEERINGEN, S. J., QUIGLEY, I., HEINZ, S., OGINO, H., OCHI, H., HELLSTEN, U., LYONS, J. B., SIMAKOV, O., PUTNAM, N., STITES, J., *ET AL*. (2016). Genome evolution in the allotetraploid frog *Xenopus laevis*. *Nature*, *538*(7625), 336-343. https://doi.org/10.1038/nature19840

THOMAS, J. O., & KORNBERG, R. D. (1975). An octamer of histones in chromatin and free in solution. *Proceedings of the National Academy of Sciences of the United States of America*, *72*(7), 2626-2630. https://doi.org/10.1073/pnas.72.7.2626

VAN ITALLIE, E., SONNETT, M., KALOCSAY, M., WÜHR, M., PESHKIN, L., & KIRSCHNER, M. W. (2025). Transitions in the proteome and phospho-proteome during *Xenopus laevis* development. *Developmental biology*, *525*, 155-171. https://doi.org/10.1016/j.ydbio.2025.05.022

VIT, G., HIRTH, A., NEUGEBAUER, N., KRAFT, B. N., SIGISMONDO, G., CAZZOLA, A., TESSMER, C., DURO, J., KRIJGSVELD, J., HOFMANN, I., BERGER, M., KLÜTER, H., NIEHRS, C., NILSSON, J., & KRÄMER, A. (2022). Human SLFN5 and its Xenopus Laevis ortholog regulate entry into mitosis and oocyte meiotic resumption. *Cell death discovery*, *8*(1), 484. https://doi.org/10.1038/s41420-022-01274-0

WARSI, S., DAHL, M., SMITH, E. M. K., RYDSTROM, A., MANSELL, E., SIGURDSSON, V., SJOBERG, J., SONEJI, S., RORBY, E., SIVA, K., GRAHN, T. H. M., LIU, Y., BLANK, U., KARLSSON, G., & KARLSSON, S. (2022). *Schlafen2* is a regulator of quiescence in adult murine hematopoietic stem cells. *Haematologica*, *107*(12), 2884-2896. https://doi.org/10.3324/haematol.2021.279799